Journal of Advanced Research Design

Tensegrity Prediction of E. coli Deactivation by Sonication Strategy

Ahmad Beng Hong Kueh[1,2,*], Isabel Lim Fong[3], Achmad Syafiuddin[4,5,6], Rosmina Ahmad Bustami[1,2]

1   Department of Civil Engineering, Faculty of Engineering, Universiti Malaysia Sarawak, 94300 Kota Samarahan, Sarawak, Malaysia
2   UNIMAS Water Centre (UWC), Faculty of Engineering, Universiti Malaysia Sarawak, 94300 Kota Samarahan, Sarawak, Malaysia
3   Department of Paraclinical Sciences, Faculty of Medicine and Health Sciences, Universiti Malaysia Sarawak, 94300 Kota Samarahan, Sarawak, Malaysia
4   Environmental Health Division, Department of Public Health, Universitas Nahdlatul Ulama Surabaya, 60237 Surabaya, Indonesia
5   Center for Environmental Health of Pesantren, Universitas Nahdlatul Ulama Surabaya, 60237 Surabaya, Indonesia
6   Department of Biomaterials, Saveetha Dental College and Hospitals, Saveetha Institute of Medical and Technical Sciences (SIMATS), Saveetha University, 600077 Chennai, India

ARTICLE INFO

ABSTRACT

Bacterial infections continue to pose a significant challenge to public health especially in clean drinking water production. Hence, it is crucial to have effective methods for their elimination. The successful deactivation of bacteria like E. coli through emerging sonic means depends on the identification of their resonant frequencies. However, the conventional approach of determining these frequencies through labor-intensive physical experimentation can be both time-consuming and expensive. This article introduces an innovative approach to determining the resonant frequency of E. coli using a specifically designed tensegrity model that incorporates spectral element formulation. This model, which conforms to the shape of E. coli, enables the calculation of resonant frequencies without the need for time-consuming simulations of element sensitivity. To address the challenges associated with rigid body motion, a small incremental operation is employed to compute the system determinant. The resonant frequencies obtained from the model are shown to align excellently with existing experimental findings. Furthermore, the model reveals that alterations in the geometry of E. coli have a substantial impact on the frequency of deactivation, while other parameters such as density have less influence. The proposed tensegrity model is a potent technique that can rapidly and accurately identify resonant frequencies, thereby enabling instantaneous and more efficient bacterial deactivation, especially during periods of health emergencies.

1. Introduction

Ensuring the security and purity of drinking water is of paramount significance for the fundamental viability of the global population. The presence of numerous illnesses resulting from water pollution caused by bacteria, viruses, and yeasts poses significant risks to human well-being, particularly in nations lacking adequate water purification infrastructure. Hence, antimicrobial activity has long been one of the chief concerns in food processing and water treatment events [1-

---

*Corresponding author.
E-mail address: kbhahmad@unimas.my

5]. Traditional approaches to water treatment in physical, chemical, or biological forms all exhibit distinct drawbacks [6-12]. For instance, techniques such as coagulation, aeration, and adsorption have been utilized to eliminate contaminants or microorganisms from water. The coagulation method involves the use of hazardous coagulants like ferric chloride, aluminum sulfate, poly aluminum chloride, poly ferric sulfate, etc., thereby posing a significant threat to water quality. The aeration approach is more challenging compared to coagulation and adsorption due to the utilization of sequencing batch reactors, which is time-consuming. Although the adsorption technique is preferred, it raises concerns about its long-term impact due to the use of toxic synthetic materials [6]. The utilization of chemicals in water treatment adds an extra burden to the management of their residuals before consumption. Hence, numerous alternatives have been suggested and continuously enhanced to address these deficiencies.

It has been revealed through academic research that the emerging method of sonification has exhibited numerous positive outcomes in the purification instances of bacterial and viral processes. This technique has proven effective in various fields including biomedicine, chemical production, consumables, energy collection and examination, beverages, and the environment, particularly in areas where maintaining clean and disinfected surroundings is of utmost significance [13,14]. Sonication is the process of disintegrating bacterial cells via the application of acoustic waves. The acoustic waves induce pressure fluctuations in the liquid medium that harbors the bacteria, thus subjecting the bacterial cells to mechanical strain. This mechanical strain can result in impairment of the cell membrane, leading to the disintegration or dissolution of the bacterial cell walls.

Typically, this process is carried out in a sonicator, a device that generates high-frequency acoustic waves in a liquid medium containing the bacteria. The utilization of sonication boasts several advantages compared to alternative methods of cell lysis, such as enhanced yields, efficient cell disintegration, and the ability to process substantial quantities of samples. In a diverse array of liquid or semi-solid samples, including food, water, and biological fluids, sonication can serve as an effective approach for deactivating bacteria. The technique has been extensively used in the cleaning of medical laboratory instruments as well as food and drink processing equipment while proven beneficial in the deactivation of microorganisms, such as Escherichia coli [15], mycobacterium sp. [16], klebsiella pneumonia [15], bacillus subtilis [17,18], Enterobacter aerogenes [17,19], Aureobasidium pullulans [17], and Microcystis aeruginosa [20], to name but a few.

Although the method of sonication is highly appealing and to some extent successful, the task of determining the appropriate frequency to deactivate the microbes or diseased cells through experimental trials has proven to be both laborious and time-consuming. Additionally, there is a lack of consensus among various studies regarding whether low or high frequencies are more effective in neutralizing these organisms. To resolve this conflict, a well-informed and systematic approach is required to identify the feasible and efficient frequency range. This issue can be narrowed down by employing a numerical or modeling approach. To achieve this, it is imperative to acquire a proficient modeling technique that possesses comprehensive knowledge in accurately characterizing the mechanics of bacteria or viruses.

The utilization of the tensegrity model is an efficient method for effectively illustrating the mechanical operations of microorganisms in a simplified fashion. The mechano-function represents the manner, in which micro living entities perceive external forces and organize themselves through modifications in intracellular biochemistry and gene expression. These reactions are then manifested through changes in their physical forms and mechanical responses [21]. The cellular tensegrity model works essentially based on a complementary alliance between the pretension forces in the living cytoskeleton that are balanced by tensile forces of the contractile actomyosin filaments, both sets of forces of which are counteracted by the intracellular contractile structures. Recent developments in

research have demonstrated the impressive potential of tensegrity models in simulating various mechanical phenomena observed in cells [14], for instance, cell migration, cell spreading, mechano-sensation, cell detachment, etc. [22].

Observing the ability to offer an accurate description of the tiny living bodies in various aspects, the tensegrity model is, therefore, employed in the current work for determining the resonant frequency of E. coli. By using this model, it is possible to determine the resonant frequency of E. coli. The calculated resonant frequency can then be used to narrow down the range necessary for deactivating E. coli using the sonication apparatus. Additionally, the proposed tensegrity model minimizes complexity as well as improves efficiency in terms of time, budget, and effort. This is especially beneficial during parametric investigations, where variations in bacteria geometry and material composition need to be considered due to their dynamic nature and uncertainties in characterization.

2. Methodology
2.1 Geometrical and Mechanical Descriptions

The single cell of E. coli is a complex biological entity that contains multiple constituents. Its principal elements consist of the cell wall, plasma membrane, cytoplasm, capsular wall, nucleoid, pili, ribosome, and flagellum. To construct the tensegrity model, the primary geometric details required are the length, diameter, and skin thickness of the cell, which is assumed to possess a rod-like shape measured from the outer capsular wall to the plasma membranes. The mechanical characterization of E. coli cells involves the consideration of the overall Young's modulus and density. The relevant geometrical and material properties for the tensegrity model are summarized in Table 1. Figure 1 illustrates the adopted tensegrity model used to simulate the E. coli cell, which is based on the triplex variant. The tensegrity model comprises 12 members, including 3 rods to withstand compressive forces, as well as top and bottom sets of triangulated 6 cables and 3 vertically inclined cables on the outer side to handle tensile forces.

Note that ρ and E_g in Table 1 are global properties measured for the whole E. coli cell. Tensegrity is a lattice-like structure [23-25], consisting of cables that resist tension and rods that handle compression. Its global properties are initially transformed into those of corresponding individual members. Subsequently, these properties are utilized to specify the material traits of the members within the tensegrity system. For brevity, Young's modulus and density of a member in the tensegrity model can be denoted, respectively, as:

$$E_m = \frac{8}{3}\frac{\pi E_g r t}{A(\sqrt{2}+4)}, \text{ and} \tag{1}$$

$$\rho_m = \frac{\rho}{16} \tag{2}$$

where *A* is the areal cross-section of each member. The coordinates of tensegrity can be determined using the following.

x-coordinates:

$$x = \left\{ r \quad -r\cos\left(\frac{\pi}{3}\right) \quad -r\cos\left(\frac{\pi}{3}\right) \quad -r\sin\left(\frac{\pi}{3}\right) \quad 0 \quad r\sin\left(\frac{\pi}{3}\right) \right\}^T \tag{3}$$

y-coordinates:

$$y = \left\{ 0 \quad r\,sin\left(\frac{\pi}{3}\right) \quad -r\,sin\left(\frac{\pi}{3}\right) \quad r\,cos\left(\frac{\pi}{3}\right) \quad -r \quad r\,cos\left(\frac{\pi}{3}\right) \right\}^T \qquad (4)$$

z-coordinates:

$$z = \left\{ 0 \quad 0 \quad 0 \quad h \quad h \quad h \right\}^T \qquad (5)$$

Table 1
Geometrical and material properties of E. coli

Property	Value	Reference
Length, h [μm]	0.3-6.0	[26-30]
Radius, r [μm]	0.25-1.0	[28,31,32]
Skin thickness, t [nm]	2-6	[33]
Density, ρ [g/mL]	0.19-1.1843	[34-36]
Young's modulus, E_g [MPa]	0.12-150	[33,37,38]
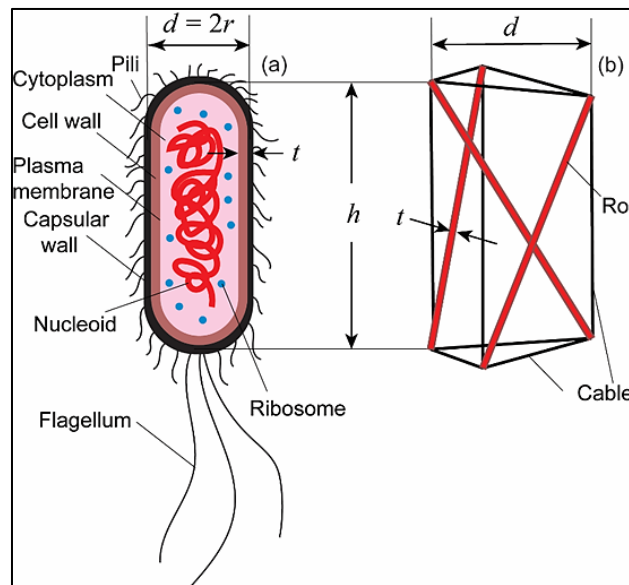
Fig. 1. (a) Schematized E. coli (b) Its tensegrity model

2.2 Spectral Element Formulation

The formulation of the tensegrity members displayed in Figure 1 is established by utilizing the spectral element technique. It has been selected due to its superiority over the finite element approach (FEA) when it comes to assessing the resonant frequency of a structure. FEA does not cover all important high-frequency wave modes unless a large number of elements is utilized through fine discretization. This limitation arises from its formulation, which relies on the frequency of independent polynomial shape functions employed [39-42]. Consequently, its accuracy is compromised, particularly at high frequencies characterized by short relevant wavelengths.

2.3 Governing Equation (Weak Form)

The governing equation for the frequency domain in its weak form is expressed as:

$$\int_0^L \delta W[-\omega^2 \rho AW - N_x W'' - F(x)]dx = 0 \tag{6}$$

Integrating by parts leads the weak form to,

$$\int_0^L [-\omega^2 \rho AW \delta W + N_x W' \delta W']dx - \delta WQ(x)|_0^L - \int_0^L \delta WF(x)dx = 0. \tag{7}$$

2.3.1 Spectral element equation

Substituting the dynamic shape functions into Eq. (7) yields,

$$\left\{\int_0^L [-\omega^2 \rho A N^T N + N_x N'^T N']dx\right\} d = (f_c + f_a), \text{ from which} \tag{8}$$

$$f_d = \int_0^L F(x)N^T(x;\omega)dx \tag{9}$$

and f_c is the spectral nodal forces vector,

$$f = \{Q_1 \quad Q_2\}^T = \{-Q(0) \quad Q(L)\}^T. \tag{10}$$

The one-element spectral equation from Eq. (8) can be expressed as:

$$S(\omega)d = f(\omega) \tag{11}$$

where,

$$S(\omega) = \int_0^L [-\omega^2 \rho A N^T N + N_x N'^T N']dx, \text{ whereas:} \tag{12}$$

$$f(\omega) = f_c(\omega) + f_d(\omega). \tag{13}$$

The spectral element is written as:

$$S(\omega) = \begin{bmatrix} S_{11} & S_{12} \\ S_{21} & S_{22} \end{bmatrix} \tag{14}$$

where,

$$S_{ij} = -N_x \alpha_{ij} - \omega^2 \rho A \beta_{ij}, \quad i, j = 1, 2, \text{ with} \tag{15}$$

$$\alpha_{11} = \frac{(k_1^2 + k_2^2)L}{(e_2 - e_1)^2}, \quad \alpha_{12} = \alpha_{21} = \frac{-(e_2 k_1^2 + e_1 k_2^2)L}{(e_2 - e_1)^2}, \quad \alpha_{22} = \frac{-(e_2^2 k_1^2 + e_1^2 k_2^2)L}{(e_2 - e_1)^2},$$

$$\beta_{11} = \frac{(e_1^2 + e_2^2)L}{(e_2 - e_1)^2}, \quad \beta_{12} = \beta_{21} = \frac{-(e_1 + e_2)L}{(e_2 - e_1)^2}, \quad \beta_{22} = \frac{2L}{(e_2 - e_1)^2}, \text{ by noting that:} \tag{16}$$

$$e_i = e^{-ik_iL}, \quad i, j = 1, 2 \text{ and} \tag{17}$$

$$k_{1,2} = \pm\omega\sqrt{\frac{\rho A}{N_x}} \tag{18}$$

2.4 Coordinates Transformation and Assembly

The conversion of the matrix equation of the spectral element from local to global definitions is executed by utilizing the coordinate transformation matrix [43-45], in which the overall system is represented as:

$$\bar{S}(\omega)\bar{d} = \bar{f}(\omega), \text{ from which} \tag{19}$$

$$\bar{S}(\omega) = T^T S(\omega) T \tag{20}$$

where $\bar{d}$ and $\bar{f}(\omega)$ are the transformed displacement and force vectors, respectively. And, the spectral elemental matrix can be written as:

$$S(\omega) = \begin{bmatrix} 0 & 0 & 0 & 0 & 0 & 0 \\ 0 & S_{11} & 0 & 0 & S_{12} & 0 \\ 0 & 0 & 0 & 0 & 0 & 0 \\ 0 & 0 & 0 & 0 & 0 & 0 \\ 0 & S_{21} & 0 & 0 & S_{22} & 0 \\ 0 & 0 & 0 & 0 & 0 & 0 \end{bmatrix} \tag{21}$$

and the transformation matrix $[T]$ is,

$$T = \begin{bmatrix} r_1 & r_2 & r_3 & 0 & 0 & 0 \\ s_1 & s_2 & s_3 & 0 & 0 & 0 \\ t_1 & t_2 & t_3 & 0 & 0 & 0 \\ 0 & 0 & 0 & r_4 & r_5 & r_6 \\ 0 & 0 & 0 & s_4 & s_5 & s_6 \\ 0 & 0 & 0 & t_4 & t_5 & t_6 \end{bmatrix} \tag{22}$$

where r_i, s_i, and t_i are the directional cosines of the local degrees of freedom relating to the global coordinate system [46]. The assembly of Eq. (19) for each member is carried out by matching the number of degrees of freedom in the global coordinate system as:

$$S_G(\omega)d_G = f_G(\omega) \tag{23}$$

The natural frequencies of the model are computed by prescribing the determinant of the global system to zero.

$$|S_G(\omega)| = 0 \tag{24}$$

A tensegrity global dynamic matrix system tends to singularity to satisfy Eq. (24) such that the common determinant calculation method can be problematic. Thus, a small incremental operation proposed by Wittrick and Williams [47] to obtain the system determinant that tends to zero is employed.

3. Results
3.1 Verification

The formulated and constructed tensegrity model is first used to compute the first natural frequency that induces resonance. This calculation is based on the geometrical and material specifications obtained from relevant literature sources. A subset of the real component of the determinant of $S_G(\omega)$ vs. frequency plot is presented in Figure 2 for E. coli studied by Li *et al.,* [48]. The resonant frequency, f_{res}, for the examined E. coli is attained from the frequency that locates the first pointy valley in the figure, i.e., $f_{res} = 20$ kHz. Table 2 lists the determined frequencies by the present tensegrity model vs. those of references [26,48,29]. It is evident that the resonant frequency utilized to deactivate various strains of E. coli, as observed in the available literature, can be accurately predicted by the present model. The level of agreement is excellent. Hence, the effectiveness of the tensegrity model is demonstrated.
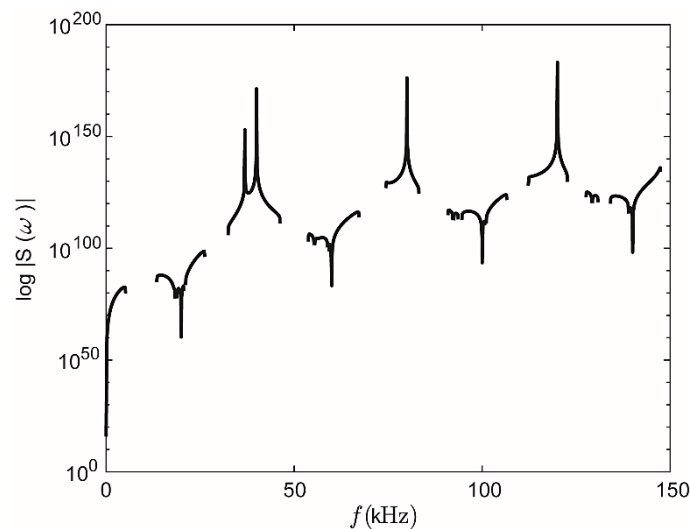
Fig. 2. Determinant of $S_G(\omega)$ vs frequency

Table 2
Verification of present tensegrity model with references

Existing work, f_{res} (kHz)	Current determination, f_{res} (kHz)	Difference (%)
20.0 [48]	20.0	0.0
20.0 [49]	20.0	0.0
30.0 [26]	30.02	0.7

3.2 Parametric Examination

The properties of E. coli cells exhibit significant variability across different sources, as evident by the data in Table 1. Consequently, it is valuable to interpret the resonant frequencies in a parametric manner, with a focus on the upper and lower bounds derived from the existing literature. An analysis of variance (ANOVA) [50,51] has been conducted for the lengths, radii, and densities obtained from these sources. Given that numerous studies consistently report an approximate global Young's modulus of 25 MPa for the cells, this parameter has been held constant.

From ANOVA, it is found that the resonant frequencies are significantly affected by the E. coli radius, r, but slightly influenced by its density, with *P*-values of 0.000 (<0.001) and 0.074 (<0.1), respectively. The squared radius term, r^2, contributes significantly also (*P*-values = 0.000 < 0.001)

while two-way interaction barely offers any significant effect (*P*-values > 0.1). The regressed equation to predict the influence of various factors takes the following form.

$$f = 227619 + 4773h - 454497r - 27.8\rho - 210hr - 4.63h\rho + 2.1r\rho + 19h^2 + 254229r^2 + 0.0141\rho^2 \qquad (25)$$

Figure 3 unveils the accuracy of the predicted *f*, f_{pred}, using Eq. (25) vs. *f* generated from varying *h*, *r*, and ρ, f_{data}, using the tensegrity model with R^2 of 0.931. Hence, a good agreement can be attained such that the regressed Eq. (25) can be used to predict the *f* of E. coli.
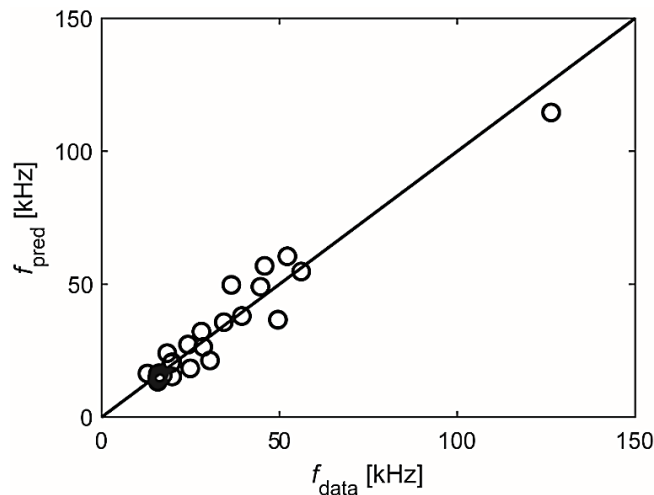
Fig. 3. *f* predicted (Eq. (25)) vs *f* determined from the tensegrity model

The effects of varying multiple factors (*h*, *r*, and ρ) on *f*, with one of the terms being fixed, can be observed in Figures 4 to 6. The ranges from Table 1 have been restricted to *h* = 0.3-4 μm, *r* = 0.25 -1 μm, ρ = 190-1184.3 fg/μm^3. Figures 4, 5, and 6 display graphs that demonstrate how the resonant frequency, *f*, of *E. coli* changes in relation to the geometric parameters *h* (height), *r* (radius), and the density ρ. Each figure contains three subplots (a, b, c) that show these relationships under different fixed conditions, allowing for an examination of each factor's impact both independently and in conjunction with others.

Figure 4 shows the relationship of the resonant frequency and the parameters *h* and ρ, with *r* kept as constants. The displayed plots in all three subplots exhibit a relatively flat configuration, i.e., *f* undergoes negligible alterations as *h* and ρ vary. This implies that within the examined ranges, *h* and ρ have limited impact on *f* when *r* is fixed. It is worth noting that as *r* increases from subplot (a) to (c), the resonant frequency surfaces remain largely flat, emphasizing the dominant role of *r* over *h* and ρ. The nearly horizontal planes further suggest that alterations in height *h* and density ρ are not sufficient to cause significant changes in the resonant frequency under fixed radius conditions.

The relationship between *f*, *r*, and ρ is illustrated in Figure 5, with *h* maintained at 0.3 μm (a), 2.15 μm (b), and 4 μm (c). The results demonstrate an inverse correlation between *r* and *f* across all graphs. The surfaces demonstrate a more pronounced gradient along the *r* axis, particularly at higher *r* values, highlighting the great impact of radius on the characterization of resonant frequency. The subtle fluctuations along the ρ axis further imply that density exerts a less pronounced effect on *f* when *h* is held constant. The rapid decline in *f* concomitant with an increase in *r* is consistent with theoretical predictions for resonant systems.
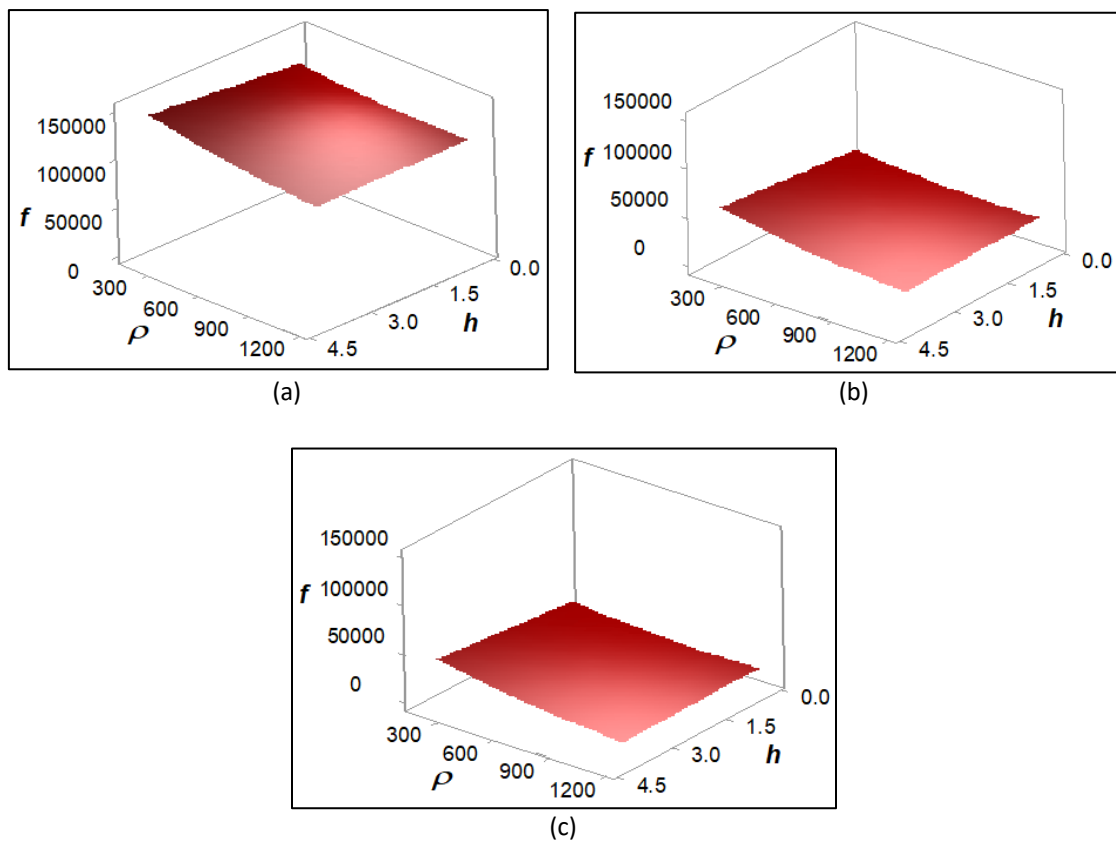
Fig. 4. Variation in the resonant frequency of E. coli for changes in *h* and ρ at E_g = 25 MPa (a) *r* = 0.25 μm (b) *r* = 0.625 μm (c) *r* = 1 μm. Note: *h* in μm, ρ in fg/μm³, and *f* in Hz in the plots
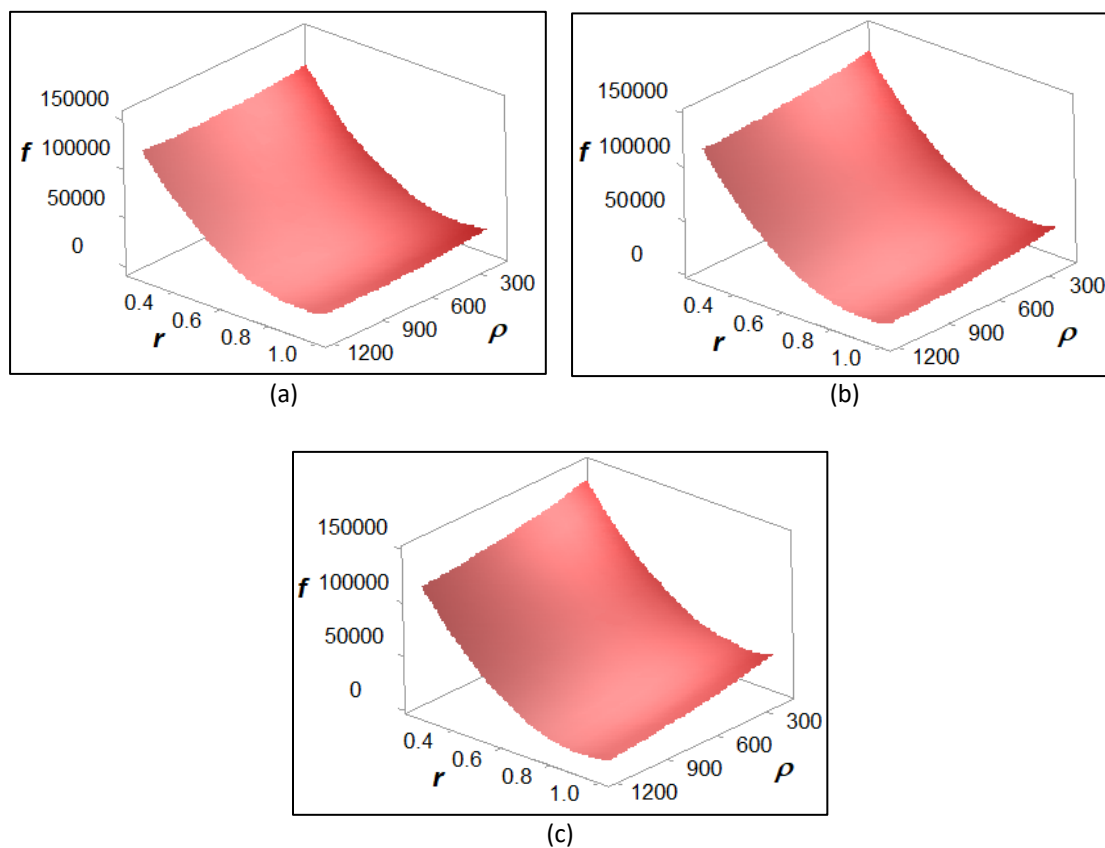
Fig. 5. Variation in the resonant frequency of E. coli for changes in *r* and ρ at E_g = 25 MPa (a) *h* = 0.3 μm (b) *h* = 2.15 μm (c) *h* = 4 μm. Note: *r* in μm, ρ in fg/μm³, and *f* in Hz in the plots
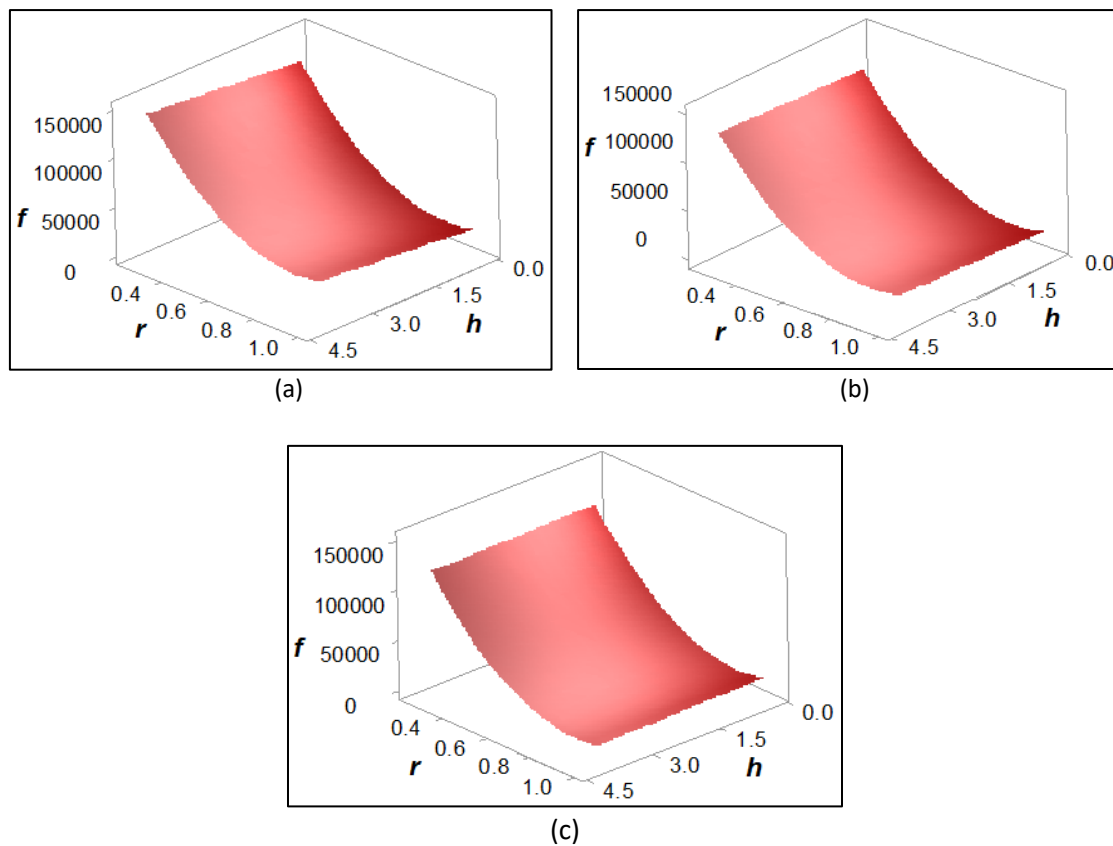
Fig. 6. Variation in the resonant frequency of E. coli for changes in *r* and *h* at E_g = 25 MPa (a) ρ = 190 fg/μm³ (b) ρ = 687.15 fg/μm³ (c) ρ = 1184.3 fg/μm³. Note: *r* and *h* in μm, and *f* in Hz in the plots

Figure 6 presents *f* as a function of *r* and *h*, with ρ kept at 190 fg/μm³, 687.15 fg/μm³, and 1184.3 fg/μm³. Consistent with Figure 5, a change in *r* leads to a reduction in *f*, thus exhibiting again the dominance of radius over both height *h* and density *ρ*. Nonetheless, in contrast to Figure 4 where *h* exhibited minimal influence, in this instance, *h* begins to demonstrate a more pronounced effect as *ρ* escalates, particularly in subplot (c). The interplay between *r* and *h* informs a rather distinctive surface configuration, wherein *f* diminishes with *r*, while the influence of *h* becomes increasingly relevant at elevated *ρ* values. This phenomenon indicates a possible interaction effect between height and density at higher ranges.

It can be conclusively seen in Figures 4 to 6 that *r* is the chief variable affecting the vibrational characteristics of E. coli, whereas *h* and *ρ* do not substantially affect *f*. This observation helps in forming a better understanding of *E. coli* and its interactions in various environmental contexts. The interaction between *r* and other factors, particularly *h* at increased *ρ* values, warrants additional examination. This analysis highlights the great necessity of optimizing *f* at numerous *E. coli* radii in practical scenarios, whereas adjustments in accordance with *h* and *ρ* may offer avenues for refinement under specific circumstances.

The primary influence of *r* on *f* can be extracted and observed in Figure 7. Again, *h* or *ρ* has comparatively little impact on the resonant frequency of E. coli. Besides, it can be inferred that *r* and *ρ* have an inverse correlation with *f*, even more so as affected by *r*. Although slightly influenced, *f* increases with *h*.
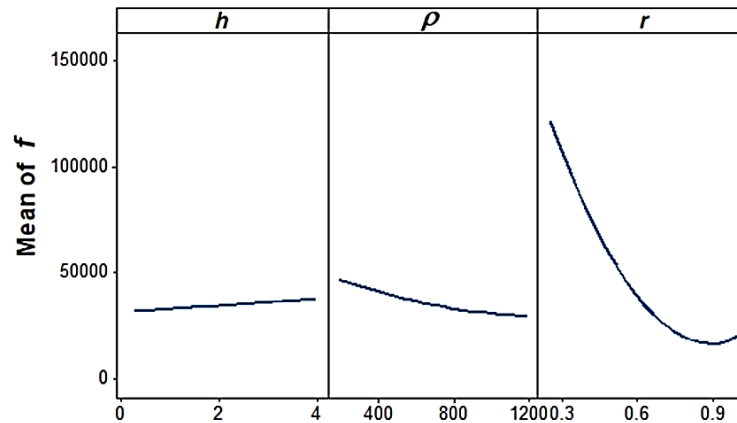
Fig. 7. Main effects of each factor on f

4. Conclusions

The spectral element formulation has been employed to numerically determine the resonant frequencies of E. coli with different geometrical and material properties using the tensegrity model. By comparing these frequencies with those reported in existing literature, it is verified that the model can accurately predict the resonant frequencies. ANOVA analysis reveals that the natural frequency of E. coli is significantly influenced by the geometrical parameter, specifically the cell radius. The density of the bacteria also contributes, albeit to a lesser extent. When the other parameters are held constant, a decrease in radius and density leads to an increase in the resonant frequency of E. coli, while an increase in height has a minimal effect. A response surface analysis has been conducted to develop a regressed equation that facilitates the prediction of the impact of various factors. It is again observed that the radius of E. coli has the most significant influence on the resonant frequency required to deactivate the bacteria. This current methodology has the potential to be extended to the treatment of other harmful bacteria in the context of drinking water, as well as the disinfection of medical and laboratory equipment.

References
[1] Shafie, Nur Fathin Amirah, Nazira Syahira Zulkifli, Roshafima Rasit Ali, Zatil Izzah Tarmizi, and Syazwani Mohd Faizo. "Green Synthesis of Titanium Dioxide Nanoparticles Using Extraction of Psidium Guajava for Smart Packaging Application." *Journal of Research in Nanoscience and Nanotechnology* 11, no. 1 (2024): 16-23. https://doi.org/10.37934/jrnn.11.1.1623

[2] Peron, Ryan Vitthaya, Amirul Ridzuan Abu Bakar, Mohd Asraf Mohd Zainuddin, Ang Qian Yee, Nik Muhammad Azhar Nik Daud, Ahmad Mukhlis Abdul Rahman, and Nurul Husna Khairuddin. "Insights into the Pharmacognostic Elucidation of Harumanis Mango (Mangifera Indica Linn.) Leaves Extracts as Therapeutic Agent." *Journal of Advanced Research in Micro and Nano Engineering* 17, no. 1 (2024): 28-41. https://doi.org/10.37934/armne.17.1.2841

[3] Dolhan, Mimi Malisa, Nur Shuhada Arbaan, and Noor Farahin Bain. "Phytoremediation of POME Using Water Lettuce and Duckweed." *Frontiers in Water and Environment* 3, no. 1 (2024): 1-8. https://doi.org/10.37934/fwe.3.1.18

[4] Naidu, Suriya Narhayhanen Rama, Shreeshivadasan Chelliapan, and Mohd Taufik Salleh. "The impact of sewage treatment plant loading to river basin during Movement Control Order." *Progress in Energy and Environment* (2023): 1-13. https://doi.org/10.37934/progee.23.1.113

[5] Chowdhury, Md Fahim Faisal, Moupia Tajrin Oyshi, and Mahbub Hasan. "Thermo-Mechanical, Structural, and Biodegradability Properties of Water Hyacinth and Sheep Wool Fiber Reinforced Hybrid Polypropylene Composites." *Malaysian Journal on Composites Science and Manufacturing* 13, no. 1 (2024): 14-24. https://doi.org/10.37934/mjcsm.13.1.1424

[6] Syafiuddin, Achmad, Salmiati Salmiati, Tony Hadibarata, Ahmad Beng Hong Kueh, Mohd Razman Salim, and Muhammad Abbas Ahmad Zaini. "Silver nanoparticles in the water environment in Malaysia: inspection, characterization, removal, modeling, and future perspective." *Scientific Reports* 8, no. 1 (2018): 986. https://doi.org/10.1038/s41598-018-19375-1

[7] Syafiuddin, Achmad, Salmiati, Tony Hadibarata, Ahmad Beng Hong Kueh, and Mohd Razman Salim. "Novel weed-extracted silver nanoparticles and their antibacterial appraisal against a rare bacterium from river and sewage treatment plan." *Nanomaterials* 8, no. 1 (2017): 9. https://doi.org/10.3390/nano8010009

[8] Loh, Zhang Zhan, Nur Syamimi Zaidi, Achmad Syafiuddin, Ee Ling Yong, Raj Boopathy, Ahmad Beng Hong Kueh, and Dedy Dwi Prastyo. "Shifting from conventional to organic filter media in wastewater biofiltration treatment: a review." *Applied Sciences* 11, no. 18 (2021): 8650. https://doi.org/10.3390/app11188650

[9] Ratnasari, Anisa, Achmad Syafiuddin, Ahmad Beng Hong Kueh, Suhartono Suhartono, and Tony Hadibarata. "Opportunities and challenges for sustainable bioremediation of natural and synthetic estrogens as emerging water contaminants using bacteria, fungi, and algae." *Water, Air, & Soil Pollution* 232, no. 6 (2021): 242. https://doi.org/10.1007/s11270-021-05183-3

[10] Ratnasari, Anisa, Nur Syamimi Zaidi, Achmad Syafiuddin, Raj Boopathy, Ahmad Beng Hong Kueh, Rizki Amalia, and Dedy Dwi Prasetyo. "Prospective biodegradation of organic and nitrogenous pollutants from palm oil mill effluent by acidophilic bacteria and archaea." *Bioresource Technology Reports* 15 (2021): 100809. https://doi.org/10.1016/j.biteb.2021.100809

[11] Mudhafar, Mustafa, Hasan Ali Alsailawi, Mohammed Zorah, Mustafa Mohammed Karhib, Ismail Zainol, and Furqan Kifah Kadhim. "Biogenic synthesis and characterization of AgNPs using CEPS: Cytotoxicity and antibacterial activites." *Journal of Advanced Research in Fluid Mechanics and Thermal Sciences* 106, no. 1 (2023): 65-75. https://doi.org/10.37934/arfmts.106.1.6575

[12] Rusli, Nur Syahirah, Mohd Nizam Lani, Sakina Shahabudin, Nina Suhaity Azmi, Elham Taghavi, Wan Zawiah Wan Abdullah, Azizah Mahmood, Anis Athirah Bahri, Suguna Migeemanathan, and Mohd Nasir Mohd Desa. "Antibiotic susceptibility and antimicrobial activity of lactic acid bacteria from malaysian fermented foods against biofilm-forming escherichia coli strains." *Journal of Advanced Research in Applied Sciences and Engineering Technology* 31, no. 1 (2023): 168-182. https://doi.org/10.37934/araset.31.1.168182

[13] Tan, Xiao, Danfeng Zhang, Keshab Parajuli, Sanjina Upadhyay, Yuji Jiang, and Zhipeng Duan. "Comparison of four quantitative techniques for monitoring microalgae disruption by low-frequency ultrasound and acoustic energy efficiency." *Environmental Science & Technology* 52, no. 5 (2018): 3295-3303. https://doi.org/10.1021/acs.est.7b05896

[14] Kueh, Ahmad BH. "Resonant frequency of coronavirus: The tensegrity approach." *Alexandria Engineering Journal* 79 (2023): 252-258. https://doi.org/10.1016/j.aej.2023.08.024

[15] Joyce, Eadaoin, A. Al-Hashimi, and Timothy J. Mason. "Assessing the effect of different ultrasonic frequencies on bacterial viability using flow cytometry." *Journal of Applied Microbiology* 110, no. 4 (2011): 862-870. https://doi.org/10.1111/j.1365-2672.2011.04923.x

[16] Al Bsoul, Abeer, Jean-Pierre Magnin, Nadine Commenges-Bernole, Nicolas Gondrexon, John Willison, and Christian Petrier. "Effectiveness of ultrasound for the destruction of Mycobacterium sp. strain (6PY1)." *Ultrasonics Sonochemistry* 17, no. 1 (2010): 106-110. https://doi.org/10.1016/j.ultsonch.2009.04.005

[17] Gao, Shengpu, Yacine Hemar, Muthupandian Ashokkumar, Sara Paturel, and Gillian D. Lewis. "Inactivation of bacteria and yeast using high-frequency ultrasound treatment." *Water Research* 60 (2014): 93-104. https://doi.org/10.1016/j.watres.2014.04.038

[18] Zou, Huasheng, and Lifang Wang. "The disinfection effect of a novel continuous-flow water sterilizing system coupling dual-frequency ultrasound with sodium hypochlorite in pilot scale." *Ultrasonics Sonochemistry* 36 (2017): 246-252. https://doi.org/10.1016/j.ultsonch.2016.11.041

[19] Gao, Shengpu, Yacine Hemar, Gillian D. Lewis, and Muthupandian Ashokkumar. "Inactivation of Enterobacter aerogenes in reconstituted skim milk by high-and low-frequency ultrasound." *Ultrasonics Sonochemistry* 21, no. 6 (2014): 2099-2106. https://doi.org/10.1016/j.ultsonch.2013.12.008

[20] Li, Yitao, Xingdong Shi, Zhi Zhang, and Yazhou Peng. "Enhanced coagulation by high-frequency ultrasound in Microcystis aeruginosa-laden water: Strategies and mechanisms." *Ultrasonics Sonochemistry* 55 (2019): 232-242. https://doi.org/10.1016/j.ultsonch.2019.01.022

[21] Ingber, Donald E., Ning Wang, and Dimitrije Stamenović. "Tensegrity, cellular biophysics, and the mechanics of living systems." *Reports on Progress in Physics* 77, no. 4 (2014): 046603. https://doi.org/10.1088/0034-4885/77/4/046603

[22] Ingber, Donald E., Laura Dike, Linda Hansen, Seth Karp, Helen Liley, Andrew Maniotis, Helen McNamee, David Mooney, George Plopper, John Sims, and Ning Wang. "Cellular tensegrity: exploring how mechanical changes in the cytoskeleton regulate cell growth, migration, and tissue pattern during morphogenesis." *International Review of Cytology* 150 (1994): 173-224. https://doi.org/10.1016/S0074-7696(08)61542-9

[23] Kueh, A. B. H., and V. T. Kho. "Strut waviness and load orientation affected fracture toughness knockdown in biaxially woven square lattices." *International Journal of Mechanical Sciences* 164 (2019): 105172. https://doi.org/10.1016/j.ijmecsci.2019.105172

[24] Kueh, A. B. H. "Fitting-free hyperelastic strain energy formulation for triaxial weave fabric composites." *Mechanics of Materials* 47 (2012): 11-23. https://doi.org/10.1016/j.mechmat.2012.01.001

[25] Kueh, Ahmad BH. "Buckling of sandwich columns reinforced by triaxial weave fabric composite skin-sheets." *International Journal of Mechanical Sciences* 66 (2013): 45-54. https://doi.org/10.1016/j.ijmecsci.2012.10.007

[26] Budari, N. M., M. F. Ali, K. H. Ku Hamid, K. A. Khalil, M. Musa, and N. F. Khairuddin. "Escherichia coli Wild Type Cells Disruption by Low Intensity Ultrasound for Bacterial Disinfection." In *InCIEC 2015: Proceedings of the International Civil and Infrastructure Engineering Conference*, pp. 21-31. Springer Singapore, 2016. https://doi.org/10.1007/978-981-10-0155-0_3

[27] Ajiboye, Timothy O., Stephen O. Babalola, and Damian C. Onwudiwe. "Photocatalytic Inactivation as a Method of Elimination of E. coli from Drinking Water." *Applied Sciences* 11, no. 3 (2021): 1313. https://doi.org/10.3390/app11031313

[28] Wu, Fabai, Aleksandre Japaridze, Xuan Zheng, Jakub Wiktor, Jacob WJ Kerssemakers, and Cees Dekker. "Direct imaging of the circular chromosome in a live bacterium." *Nature Communications* 10, no. 1 (2019): 2194. https://doi.org/10.1038/s41467-019-10221-0

[29] Nurliyana, M. R., M. Z. Sahdan, K. M. Wibowo, A. Muslihati, H. Saim, S. A. Ahmad, Y. Sari, and Z. Mansor. "The detection method of Escherichia coli in water resources: A review." In *Journal of Physics: Conference Series*, vol. 995, p. 012065. IOP Publishing, 2018. https://doi.org/10.1088/1742-6596/995/1/012065

[30] Gammoudi, Ibtissem, Marion Mathelie-Guinlet, Fabien Morote, Laure Beven, Daniel Moynet, Christine Grauby-Heywang, and Touria Cohen-Bouhacina. "Morphological and nanostructural surface changes in Escherichia coli over time, monitored by atomic force microscopy." *Colloids and Surfaces B: Biointerfaces* 141 (2016): 355-364. https://doi.org/10.1016/j.colsurfb.2016.02.006

[31] Odonkor, Stephen T., and Joseph K. Ampofo. "Escherichia coli as an indicator of bacteriological quality of water: An overview." *Microbiology Research* 4, no. 1 (2013): e2. https://doi.org/10.4081/mr.2013.e2

[32] Cui, Qianqian, Tianqing Liu, Xiangqin Li, Lidan Zhao, Qiqi Wu, Xin Wang, Kedong Song, and Dan Ge. "Validation of the mechano-bactericidal mechanism of nanostructured surfaces with finite element simulation." *Colloids and Surfaces B: Biointerfaces* 206 (2021): 111929. https://doi.org/10.1016/j.colsurfb.2021.111929

[33] Gumbart, James C., Morgan Beeby, Grant J. Jensen, and Benoît Roux. "Escherichia coli peptidoglycan structure and mechanics as predicted by atomic-scale simulations." *PLoS Computational Biology* 10, no. 2 (2014): e1003475. https://doi.org/10.1371/journal.pcbi.1003475

[34] Lewis, Christina L., Caelli C. Craig, and Andre G. Senecal. "Mass and density measurements of live and dead gram-negative and gram-positive bacterial populations." *Applied and Environmental Microbiology* 80, no. 12 (2014): 3622-3631. https://doi.org/10.1128/AEM.00117-14

[35] Martinez-Salas, E., J. A. Martin, and M. Vicente. "Relationship of Escherichia coli density to growth rate and cell age." *Journal of Bacteriology* 147, no. 1 (1981): 97-100. https://doi.org/10.1128/jb.147.1.97-100.1981

[36] Shiloach, Joseph, and Rephael Fass. "Growing E. coli to high cell density—a historical perspective on method development." *Biotechnology advances* 23, no. 5 (2005): 345-357. https://doi.org/10.1016/j.biotechadv.2005.04.004

[37] Tuson, Hannah H., George K. Auer, Lars D. Renner, Mariko Hasebe, Carolina Tropini, Max Salick, Wendy C. Crone, Ajay Gopinathan, Kerwyn Casey Huang, and Douglas B. Weibel. "Measuring the stiffness of bacterial cells from growth rates in hydrogels of tunable elasticity." *Molecular Microbiology* 84, no. 5 (2012): 874-891. https://doi.org/10.1111/j.1365-2958.2012.08063.x

[38] Kandemir, Nehir, Waldemar Vollmer, Nicholas S. Jakubovics, and Jinju Chen. "Mechanical interactions between bacteria and hydrogels." *Scientific Reports* 8, no. 1 (2018): 10893. https://doi.org/10.1038/s41598-018-29269-x

[39] Koo, S. Q., and A. B. H. Kueh. "Finite Element State-Space Model of Edge Initiating Localized Interfacial Degeneration of Damped Composite Laminated Plates." In *IOP Conference Series: Materials Science and Engineering*, vol. 620, no. 1, p. 012072. IOP Publishing, 2019. https://doi.org/10.1088/1757-899X/620/1/012072

[40] Drahman, Siti Hasyyati, Ahmad Beng Hong Kueh, and Ahmad Razin Zainal Abidin. "Low-velocity impact of composite sandwich plate with facesheet indentation description." *Jurnal Teknologi* 77, no. 16 (2015). https://doi.org/10.11113/jt.v77.6383

[41] Kam, Chee Zhou, and Ahmad Beng Hong Kueh. "Bending Response of Cross-Ply Laminated Composite Plates with Diagonally Perturbed Localized Interfacial Degeneration." *The Scientific World Journal* 2013, no. 1 (2013): 350890. https://doi.org/10.1155/2013/350890

[42] Abo Sabah, Saddam Hussein, and Ahmad Beng Hong Kueh. "Finite element modeling of laminated composite plates with locally delaminated interface subjected to impact loading." *The Scientific World Journal* 2014, no. 1 (2014): 954070. https://doi.org/10.1155/2014/954070

[43] Kueh, A. B. H. "Thermally-induced responses of triaxially woven fabric composites." *Heliyon* 9, no. 7 (2023). https://doi.org/10.1016/j.heliyon.2023.e17631

[44] Al-Fasih, M. Y., A. B. H. Kueh, SH Abo Sabah, and M. Y. Yahya. "Influence of tows waviness and anisotropy on effective Mode I fracture toughness of triaxially woven fabric composites." *Engineering Fracture Mechanics* 182 (2017): 521-536. https://doi.org/10.1016/j.engfracmech.2017.03.051

[45] Al-Fasih, M. Y., A. B. H. Kueh, and M. H. W. Ibrahim. "Failure behavior of sandwich honeycomb composite beam containing crack at the skin." *Plos one* 15, no. 2 (2020): e0227895. https://doi.org/10.1371/journal.pone.0227895

[46] Rasin, Norhidayah, Ahmad BH Kueh, Muhammad NH Mahat, and Airil Y. Mohd Yassin. "Stability of triaxially woven fabric composites employing geometrically nonlinear plate model with volume segmentation ABD constitution." *Journal of Composite Materials* 50, no. 19 (2016): 2719-2735. https://doi.org/10.1177/0021998315612538

[47] Wittrick, W_H, and FW2890000227 Williams. "A general algorithm for computing natural frequencies of elastic structures." *The Quarterly Journal of Mechanics and Applied Mathematics* 24, no. 3 (1971): 263-284. https://doi.org/10.1093/qjmam/24.3.263

[48] Li, Jiao, Luyao Ma, Xinyu Liao, Donghong Liu, Xiaonan Lu, Shiguo Chen, Xingqian Ye, and Tian Ding. "Ultrasound-induced Escherichia coli O157: H7 cell death exhibits physical disruption and biochemical apoptosis." *Frontiers in Microbiology* 9 (2018): 2486. https://doi.org/10.3389/fmicb.2018.02486

[49] Liao, Xinyu, Jiao Li, Yuanjie Suo, Shiguo Chen, Xingqian Ye, Donghong Liu, and Tian Ding. "Multiple action sites of ultrasound on Escherichia coli and Staphylococcus aureus." *Food Science and Human Wellness* 7, no. 1 (2018): 102-109. https://doi.org/10.1016/j.fshw.2018.01.002

[50] Kueh, A. B. H. "Artificial neural network and regressed beam-column connection explicit mathematical moment-rotation expressions." *Journal of Building Engineering* 43 (2021): 103195. https://doi.org/10.1016/j.jobe.2021.103195

[51] Kueh, A. B. H., A. W. Razali, Y. Y. Lee, S. Hamdan, I. Yakub, and N. Suhaili. "Acoustical and mechanical characteristics of mortars with pineapple leaf fiber and silica aerogel infills–Measurement and modeling." *Materials Today Communications* 35 (2023): 105540. https://doi.org/10.1016/j.mtcomm.2023.105540